Journal of Magnetism and Magnetic Materials 353 (2014) 23–28

Contents lists available at ScienceDirect

Journal of Magnetism and Magnetic Materials

journal homepage: www.elsevier.com/locate/jmmm

Magnetic and dielectric properties of the $PbFeBO_4$ single crystal

A. Pankrats*, K. Sablina, D. Velikanov, A. Vorotynov, O. Bayukov, A. Eremin, M. Molokeev, S. Popkov, A. Krasikov

Kirensky Institute of Physics SB RAS, 660036 Krasnoyarsk, Russia

ARTICLE INFO

Article history:
Received 17 April 2013
Available online 18 October 2013

Keywords:
Single crystal growth
Magnetic susceptibility
Magnetic phase transition
Antiferromagnetic order
Dielectric permittivity
Magnetoelectric effect

ABSTRACT

$PbFeBO_4$ single crystals up to $4 \times 2.5 \times 0.5$ mm^3 in size were grown by spontaneous crystallization from a solution in a melt and their magnetic and dielectric properties were investigated. The high Neel temperature $T_N = 114$ K and the absence of the broad maximum of susceptibility above the Neel temperature suggest that the $PbFeBO_4$ crystal is a three-dimensional antiferromagnet. The magnetic susceptibility anisotropy in the ordered state indicates that the antiferromagnetic vector is directed along the orthorhombic ***c*** axis. The anomalies of dielectric permittivities ε' and ε'' were observed in both polycrystalline and single-crystal samples within the temperature ranges where the short- and long-range magnetic orders are established. This confirms the correlation between the magnetic and electric subsystems in the crystal.

1. Introduction

The search for new or magnetically unexplored oxide compounds with a sufficient number of magnetic ions of the iron group involves the study of their crystal structure and the possibility of growing single crystals of these materials. Natural minerals with diverse crystal structures are an inexhaustible source of the crystals interesting for physics of magnetic phenomena. Wide opportunities are opened by using matrices of the elements that allow isomorphic substitution with embedding paramagnetic ions.

The study of the properties of natural materials is often complicated by the presence of various impurities and requires synthesizing pure analogs. It is preferable to investigate single crystals of materials because of their higher purity. The purest single crystals are obtained when their chemical composition includes potential solvents, such as PbO, B_2O_3, and Bi_2O_3 oxides or their combinations. Using the pseudo-flux method, we succeeded in growing Bi_2CuO_4 [1], CuB_2O_4 [2], $Cu_5Bi_2B_4O_{14}$ [3], $Pb_2Fe_2Ge_2O_9$ [4], and other single crystals. Investigations carried out on single-crystal samples yield more information on characteristics of the materials. As is known, some compounds exhibit the discrepancy in magnetic behaviors of single-crystal and polycrystalline samples. For example, the temperatures of the magnetic phase transition in polycrystalline $MnGeO_3$ lie within $T_N = 10$–16 K, while in the single-crystal $MnGeO_3$ sample the transition occurs at $T_N = 36$ K [5].

In this study, we investigate first the magnetic and dielectric properties of the $PbFeBO_4$ in the single crystal state. The magnetic properties of polycrystalline $PbMBO_4$ (M = Mn, Cr, Fe) were reported in [6], where the temperature of the magnetic phase transition in $PbFeBO_4$ was found to be $T_N \approx 120$ K, which is much higher than that in the crystals with M = Mn and Cr. In the temperature dependence of the magnetic susceptibility for polycrystalline $PbFeBO_4$, there is a broad peak at 280 K, which was attributed to the establishment of the short-range antiferromagnetic order in the one-dimensional chains of oxygen octahedra containing iron ions. This explanation, however, seems to us unconvincing, considering the excessively high value of the magnetic phase transition temperature for a quasi-one-dimensional magnet.

The strong difference between the magnetic properties of $PbFeBO_4$ and those of other compounds in this family stimulated the interest in the thorough investigation of this material. In addition, $PbFeBO_4$ contains Pb^{2+} ions with a stereochemical feature; the unusual distribution of the electron density related to outer $6s^2$ electrons that do not participate in the formation of a chemical bond and create isolated pairs (lone pairs). These pairs strongly affect ionic coordination and can lead to the occurrence of ferroelectric, nonlinear optical, and other interesting properties of the compound.

To investigate the magnetic and dielectric properties of $PbFeBO_4$ in more detail, we grew single crystals of this compound. The results obtained showed that the magnetic behaviors of the material in the single-crystal and polycrystalline states are strongly different. In the temperature ranges where the short- and long-range magnetic orders are established, the anomalies of the dielectric properties of the polycrystalline and single-crystal samples were observed, which indicates the correlation between the magnetic and electrical subsystems in the crystal.

* Correspondence to: Kirensky Institute of Physics SB RAS, 50 Akademgorodok, bld. 38, 660036 Krasnoyarsk, Russia. Tel.: +7 391 290 71 08.
E-mail addresses: pank@iph.krasn.ru, a.pankrats@mail.ru (A. Pankrats).

0304-8853/$ - see front matter © 2013 Elsevier B.V. All rights reserved.
http://dx.doi.org/10.1016/j.jmmm.2013.10.018

2. Material and methods

2.1. Crystal growth

$PbFeBO_4$ single crystals were grown by spontaneous crystallization from a solution in a melt. The eutectic composition in the system $PbO–B_2O_3$ (93.7 wt% PbO and 6.3 wt% B_2O_3) with the melting point $T_m=460$ °C [7] was used as a solvent. The fully mixed composition 13.42 g PbO + 2.08 g B_2O_3 + 2.31 g Fe_2O_3 was placed into a platinum crucible and heated to 1000 °C. After exposure at this temperature for 2 h, the furnace with the crucible was cooled at a rate of 10 °C/h to $T=500$ °C. The crystals were mechanically withdrawn from the crucible. The crystals with a maximum size of $4\times2.5\times0.5$ mm^3 had a prismatic form. The smallest crystals (less than 1 mm in size) were green and transparent.

2.2. X-ray data

The crystal structure of the samples was determined on a D8 ADVANCE X-ray powder diffractometer (Bruker). It was confirmed that the structure is described by the orthorhombic space group Pnma, $Z=4$; the measured lattice constants $a=7.00$ Å, $b=5.94$ Å, and $c=8.33$ Å are in good agreement with those reported in [6,8] for $PbFeBO_4$ and $PbGaBO_4$. The crystal structure (Fig. 1) consists of infinite chains of the edge-shared FeO_6 octahedra extended along the ***b*** axis. The chains are bridged by the orthoborate groups BO_3 forming the three-dimensional $FeBO_4^{2-}$ framework. The Pb^{2+} cations occupy asymmetric 4-fold coordination sites typical of the stereoactive pairs with s-orbitals and fill the empty [010] tunnels in the structure.

Orientation of the single crystals was investigated using a SMART APEX II automated X-ray single-crystal diffractometer (Bruker). The data obtained showed no twinning and confirmed high crystal quality of the samples. The largest size of the plate-like sample coincides with the orthorhombic ***b*** axis and the plate plane is crystallographic (101).

2.3. Experimental methods

The magnetic properties of the crystal were studied using an MPMS SQUID magnetometer (Quantum Design) in magnetic fields up to 50 kOe at temperatures of 2–300 K. Additional measurements were performed using a vibrating sample magnetometer (VSM) in magnetic fields up to 90 kOe and in pulse magnetic fields up to 280 kOe.

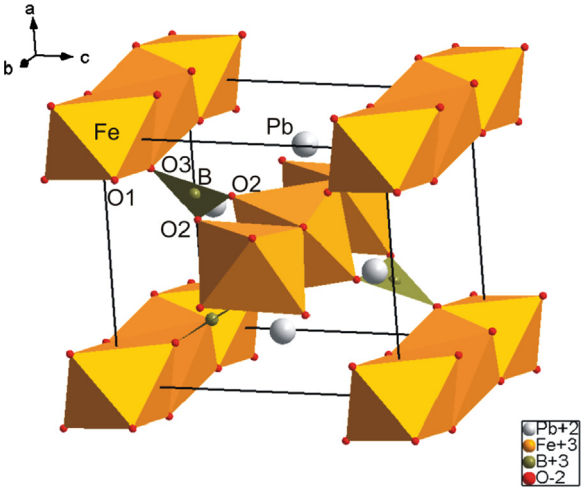

Fig. 1. Crystal structure of $PbFeBO_4$.

The dielectric properties of the samples were determined on an Agilent E4980A LCR-meter in the frequency range from 10 kHz to 2 MHz. The investigated samples were a polycrystalline pill 5 mm in diameter sintered from grinded single crystals and the single crystal $1.7\times1.1\times0.5$ mm^3 in size. The electrodes were formed from a silver paste deposited onto the pill faces or the largest faces of the single crystal that coincide with the orthorhombic (101) planes.

Mössbauer spectra of $PbFeBO_4$ were obtained on an MS1104Em spectrometer using a ^{57}Co (Cr) source at room temperature.

3. Results

High quality of the $PbFeBO_4$ single crystals is confirmed by both the X-ray study and the Mössbauer spectroscopy. The Mössbauer spectrum of the crystal is presented in Fig. 2a. At room temperature, the spectrum consists of two doublets shown by arrows. The intensity of one of them is higher than the intensity of the other by two orders of magnitude. The probability distribution of quadrupole splitting (QS) shows that there are only two iron positions in the sample (Fig. 2b). The fitting of the two-doublet model spectrum to the experimental data yields the Mössbauer parameters for two positions of iron ions (Table 1).

Judging by the value of the isomer chemical shift (IS) 0.33 mm/s, most of iron ions (site 1) are in the high-spin trivalent state and occupy the octahedral sites. A relatively high value of QS (1.62 mm/s) indicates strong distortion of the coordination octahedra around iron.

An insignificant fraction of Fe ions (no more than 2%) that can be associated with the surface states or defects in the crystal structure (site 2) are also in the high-spin trivalent state. However, the value of QS for these ions is much higher than that for most of iron; i.e., the octahedral surrounding is distorted stronger.

Temperature dependences of the magnetic susceptibility for the $PbFeBO_4$ single crystal measured along all the orthorhombic crystal axes in a magnetic field of 5 kOe are presented in Fig. 3. The temperature of the magnetic phase transition $T_N=114$ K is determined by the jump of the derivative $d\chi/dT$ at $H\|\boldsymbol{c}$ (see inset in Fig. 3) and the sharp susceptibility peak at $H\|\boldsymbol{b}$. The Neel temperature is slightly lower than that reported in [6].

Field dependences of magnetization of $PbFeBO_4$ measured along all the orthorhombic axes at different temperatures are shown in Fig. 4. For all the crystal orientations, the magnetization depends linearly on a magnetic field. According to the temperature dependences of susceptibility (Fig. 3), the field dependences of magnetization slightly change with temperature for all the magnetic field directions, except for $H\|\boldsymbol{c}$.

The electron spin resonance (ESR) spectra of the single-crystal samples taken from different parts of the crucible were studied in the temperature range 140–300 K using an Elexsyss E580 X-band spectrometer (Bruker). Fig. 5 presents typical ESR spectra for samples 1 and 2 at room temperature and an arbitrary chosen orientation in the ***ac*** plane. The spectra consist of two lines: broad line A with $\Delta H=4500$–6500 Oe and $H_r\approx3800$ Oe and narrow line B with $\Delta H\approx200$ Oe and $H_r\approx3200$ Oe (*2* in Fig. 6). It should be noted that the intensities of lines A and B differ by $\sim10^3$. In addition, the intensities of the narrow line for different samples significantly vary. Upon sample cooling, this line acquires a fine structure with four weaker peaks symmetric with respect to the central line. The inset of Fig. 5 demonstrates the fragment of the resonance spectrum for sample 2 where the arrows show the lines related to the fine structure of the spectrum. This part of the spectrum can be attributed to the single-ion ESR spectrum for an ion with the spin $S=5/2$. This spectrum is most likely associated with isolated Fe^{3+} ions, which are not coupled with iron ions of the main part of the crystal by the exchange interaction. It is

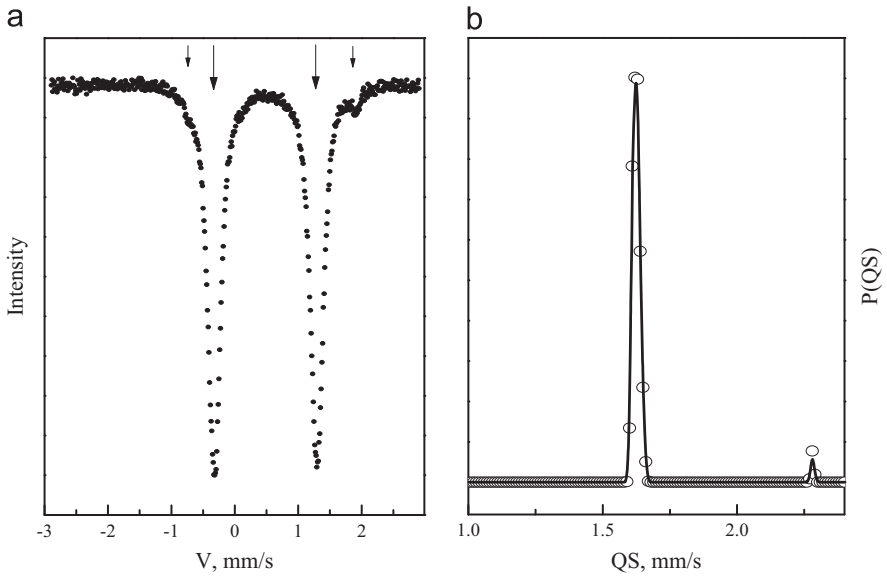

Fig. 2. (a) Mössbauer spectrum of $PbFeBO_4$ at room temperature, (b) probability distribution of quadrupole splitting.

Table 1
Mössbauer parameters for two positions of iron ions.

Site number	Isomeric chemical shift IS, mm/s	Quadrupole splitting QS, mm/s	Linewidth, mm/s	Site population
1	0.33	1.62	0.23	0.98
2	0.44	2.65	0.09	0.02

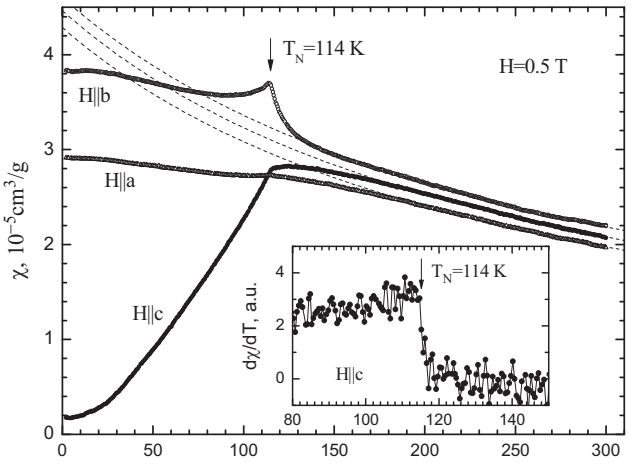

Fig. 3. Temperature dependences of the magnetic susceptibility for the $PbFeBO_4$ single crystal. Inset: temperature dependence of the derivative $d\chi/dT$ at $H \| \boldsymbol{c}$.

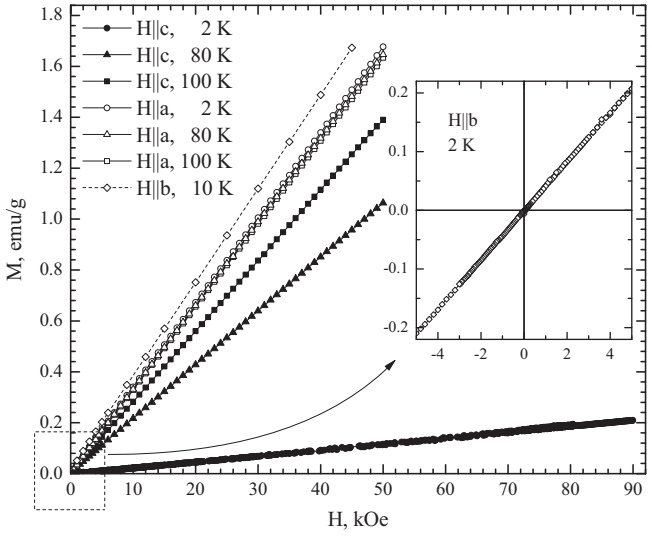

Fig. 4. Field dependences of magnetization of $PbFeBO_4$ measured along all the orthorhombic axe Inset: the portion of field dependences of magnetization in ***b*** direction at $T=2$ K.

reasonable to suggest that the isolated Fe^{3+} ions cause the above-mentioned additional doublet in the Mössbauer spectrum of the crystal. Fig. 6 shows the temperature dependence of the A linewidth for sample 2 measured at the same field orientation as in Fig. 5. The sharp broadening of line A on approaching the Neel temperature unambiguously associates this line with the resonance absorption in the $PbFeBO_4$ crystal volume.

The synthesized $PbFeBO_4$ crystals are good insulators. Their electrical resistance at room temperature exceeds $10^{12}\,\Omega$. The dielectric properties of $PbFeBO_4$ were studied on both polycrystalline and single-crystal samples. Fig. 7 shows temperature dependences of real and imaginary permittivity parts ε' and ε'' measured at different frequencies on the polycrystalline sample. At all the frequencies, as the decreasing temperature approaches temperature T_N of the magnetic phase transition (shown by the arrow in Fig. 7), real permittivity part ε' grows. With an increase in the measuring frequency, the anomaly noticeably broadens. A sharp increase in imaginary permittivity part ε'' is observed in the same temperature range. Another anomaly in the behavior of ε' and ε'' is observed at higher temperatures. Its position strongly depends on frequency and shifts towards higher temperatures as the frequency is increased.

The dielectric properties of the $PbFeBO_4$ single crystal were measured in the same temperature and frequency ranges as those of the polycrystalline sample. However, in this case, the calculation of the true values of ε' and ε'' is inaccurate because of a small size of the single crystal. Moreover, at such a sample size it is impossible to apply the thin plate capacitor approximation. For this reason, we present only temperature dependences of capacitance C and dielectric loss tg δ (Fig. 8), which allow us to compare qualitatively the dielectric properties of the polycrystalline and single-crystal samples. The comparison shows that the anomalies of the dielectric properties described for the polycrystalline sample remain in the

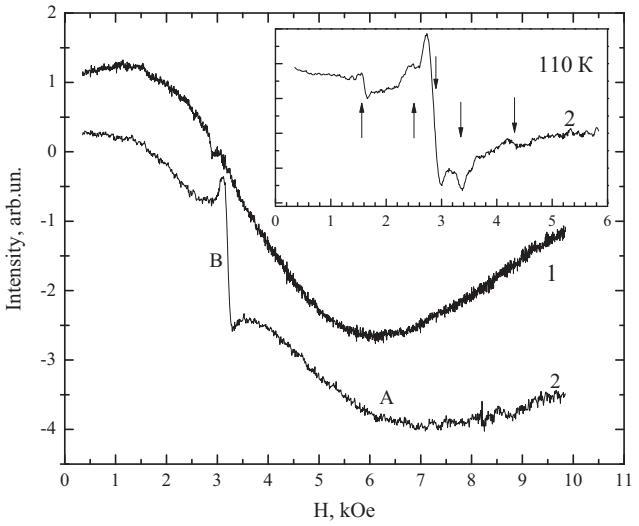

Fig. 5. ESR spectra for samples 1 and 2 at room temperature. Inset: the portion of ESR spectrum for sample 2 at $T=110$ K.

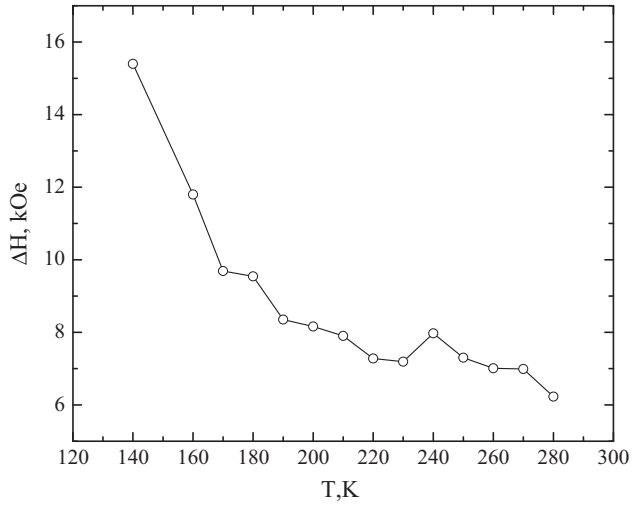

Fig. 6. Temperature dependence of the A linewidth for sample 2.

case of the single crystal. Similar to the polycrystalline sample, a sharp increase in the capacitance and dielectric loss near the Neel temperature is observed for the single crystal. The dielectric loss grows with temperature approaching T_N. The observed anomalies shift towards higher temperatures as the frequency is increased. At the same time, the high-temperature anomaly of the capacitance is much weaker for the single crystal than for the polycrystalline sample.

4. Discussion

Having analyzed the magnetic measurement data, we note the absence of the high-temperature broad maximum of susceptibility observed in the polycrystalline samples at $T\approx 280$ K [6]. The authors attributed this anomaly to the establishment of the short-range magnetic order in 1D infinite chains of the edge-shared FeO_6 octahedra. At the same time, the authors admitted the presence of some amount of the hematite phase in the polycrystalline samples. The hematite α-Fe_2O_3 is a rhombohedral antiferromagnet with the Neel temperature $T_N=950$ K [9]. As is known, α-Fe_2O_3 undergoes the Morin spin–reorientation transition between the low-temperature collinear antiferromagnetic and

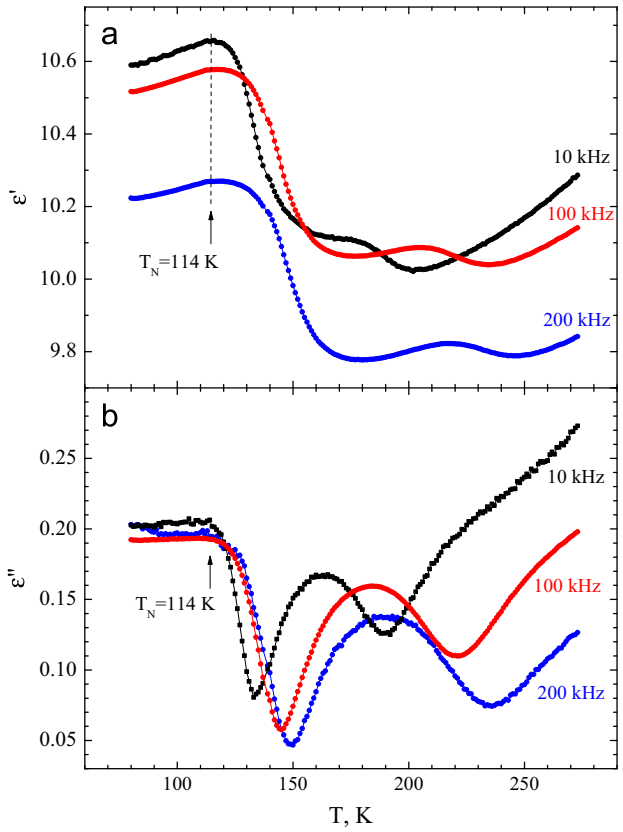

Fig. 7. Temperature dependences of real and imaginary permittivity parts ε' and ε'' measured at different frequencies on the polycrystalline sample.

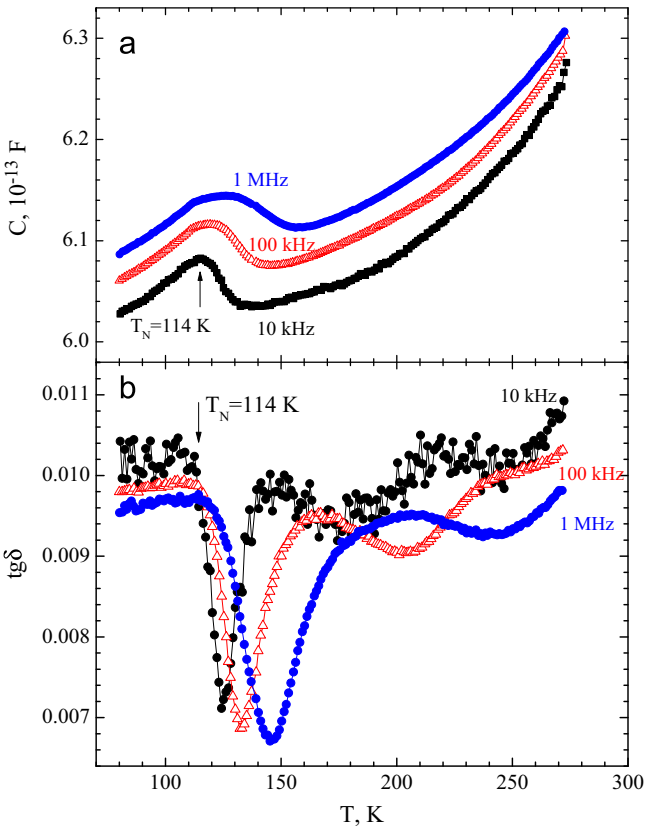

Fig. 8. Temperature dependences of capacitance (a) and dielectric loss tg δ (b) measured at different frequencies on the single crystal.

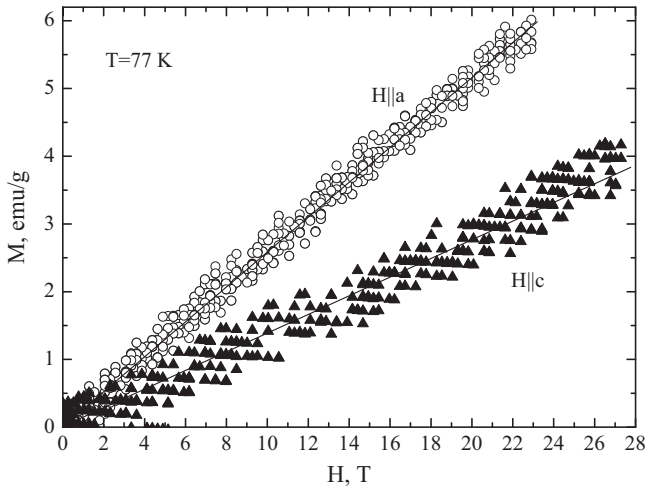

Fig. 9. Field dependences of magnetization of $PbFeBO_4$ measured along *a* and *c* orthorhombic axes at $T=77$ K.

high-temperature weak ferromagnetic states at $T_M \approx 260$ K. Thus, it is reasonable to suggest that the susceptibility maximum starting at $T \approx 250$ K [6] is induced by spontaneous magnetization of the impurity hematite phase at the Morin transition.

The study of the magnetic properties of the $PbFeBO_4$ single crystal shows that the magnetic susceptibilities are described well by the Curie-–Weiss law in the temperature range 170–300 K along all the orthorhombic crystal axes. The curves are shown by dashed lines in Fig. 4. The effective magnetic moments are $\mu_{a,eff}=5.47$, $\mu_{b,eff}=5.83$ and $\mu_{c,eff}=5.65$ in Bohr magneton. These values are close to the theoretical value $\mu_{eff}=5.92$ for a Fe^{3+} ion. The paramagnetic Curie temperatures are $\theta_a=-256$ K, $\theta_b=-272$ K, and $\theta_c=-262$ K, which amounts to the doubled Neel temperatures.

As is known, the temperature of the Morin transition in hematite is highly sensitive to pressure [10], substitution of other ions for Fe^{3+} [11–14], and other factors affecting the magnetic anisotropy of the crystal. Most of these factors decrease T_M. The same effect is caused by a decrease in the hematite crystal size [15]. Microcrystallites can be in the weak ferromagnetic state down to very low temperatures. Thus, the spontaneous magnetic moment of the weak ferromagnetic state of the impurity hematite phase can cause another magnetic peculiarity of the polycrystalline $PbFeBO_4$ samples [6], specifically, the large difference in the susceptibilities measured upon cooling the sample in a magnetic field and without it in the wide temperature range from 2 to 350 K. In our measurements performed on the single crystal, no dependence of the magnetic susceptibility on the magnetic prehistory of the sample is observed.

In the ***b*** axis direction, there is a sharp magnetic susceptibility peak at the Néel temperature in magnetic fields up to 5T, which is absent for the other directions. Such peaks were observed in some canted antiferromagnets with weak ferromagnetism (see, for example, [16]). The maximum susceptibility defined as the derivative $\chi=dM/dH$ was found only in the crystallographic direction where there is weak ferromagnetism and was caused by the occurrence of the spontaneous magnetic moment at the magnetic phase transition. Our data shown in Fig. 4 correspond to the susceptibility defined as $\chi=M/H$. Moreover, the thorough measurements of field dependences of magnetization in this direction (see inset in Fig. 4) showed that there is no weak ferromagnetism in this crystal. The similar susceptibility peak was observed at the magnetic phase transition in polycrystalline $NaMn_7O_{12}$ [17], where it was explained by the Hopkinson effect. This explanation, however, seems unconvincing in case of the $PbFeBO_4$ and $NaMn_7O_{12}$ antiferromagnets, since the Hopkinson effect is significant only for ferromagnets. The reason for the sharp peak susceptibility in the b axis direction of $PbFeBO_4$ is still unclear.

The anisotropy of the magnetic susceptibility is observed even in the paramagnetic region where it is most likely caused by the anisotropy of the *g*-factor. Unfortunately, since resonance line A is very broad due to the resonant absorption in the crystal volume, we cannot measure the anisotropy of the g factor directly from the ESR data. Below the Neel temperature, the anisotropy of the magnetic susceptibility is significant; the susceptibility measured along the c axis tends to zero at low temperatures and remains almost invariable for the other measurement directions. This behavior indicates that the orthorhombic ***c*** axis is the easy-magnetization axis of the antiferromagnet, which confirms the $PbFeBO_4$ magnetic structure based on the results of the neutron study [6].

In the field dependence of the magnetization in the easy direction, the spin-flop transition should be observed; however, it was not found at $T=4.2$ K in the maximum attainable in our experiment the static magnetic field up to 90 kOe (Fig. 4). The critical field of the transition usually grows with temperature, which corresponds to the decreasing difference between the magnetic susceptibilities along the easy axis and perpendicular to it (Fig. 3). We measured the field dependences of the magnetization in these two directions in pulse magnetic fields at $T=77$ K (Fig. 9). The spin-flop transition is not found in fields up to 280 kOe. The broader data spread in the easy direction ***c*** is due to the weaker desired signal for this direction as compared with electromagnetic noise. Due to the strong critical fields of the spin-flop transition and, consequently, large energy gaps of the AFMR spectrum, we did not find the AFMR resonance absorption in the crystal at frequencies up to 140 GHz.

The susceptibility $\chi=3.35\times10^{-5}$ cm^3/g at $T=2$ K calculated from the field dependence of magnetization for the orthorhombic ***b*** axis allows us to estimate the effective exchange field at this temperature $H_E=1.3\times10^6$ Oe. This value is typical of a three-dimensional antiferromagnet.

The study of the dielectric properties of the polycrystalline and single-crystal $PbFeBO_4$ samples shows the anomalous behavior of the real and imaginary permittivity parts due to magnetoelectric effect in two temperature ranges. The low-temperature anomalies near the Neel temperature are obviously due to the established long-range antiferromagnetic order, while the high-temperature anomalies are most likely associated with the short-range magnetic order in the crystal. Thus, in the $PbFeBO_4$ crystal, the dielectric properties correlate with the magnetic order.

The permittivity anomalies at the magnetic phase transition were observed in a number of antiferromagnets: $Bi_2Fe_4O_9$ [18], $TeCuO_3$ [19], $RMnO_3$[20], etc. We cannot state that such anomalies characterize $PbFeBO_4$ and the similar crystals as multiferroics with coexisting spontaneous polarization and magnetic ordering. Anyhow, we failed to identify the electric polarization in $PbFeBO_4$ by measuring the polarization current at temperatures below T_N in both the polycrystalline and single-crystal states. However, the absence of the polarization current in our experiment is not an unambiguous result. In crystals, the polarization current can be observed only at certain electric field orientations relative to the crystallographic axes (see, for example, [18]). For this reason, in the polycrystalline sample the polarization current can be weakened due to averaging overall possible crystallite directions. On the other hand, the pronounced plate-like shape of the $PbFeBO_4$ single crystals allowed us to perform the measurements only in the $E\|[101]$ direction. Therefore, at present we try to grow larger crystals to measure the polarization current in the other electric field directions.

At the same time, a noticeable dependence of the dielectric properties on a *dc* magnetic field of 10 kOe applied parallel to the *ac* electric field was detected for neither the polycrystalline nor

single crystal sample. Probably, one should not expect any significant magnetoelectric response in antiferromagnets with the strong exchange interaction in external magnetic fields weaker than the exchange field [21].

5. Conclusions

$PbFeBO_4$ single crystals up to $4 \times 2.5 \times 0.5$ mm^3 in size were grown and their magnetic and dielectric properties were investigated. The magnetic behavior of the single-crystal $PbFeBO_4$ differs strongly from that of polycrystalline one. The paramagnetic susceptibility of the crystal obeys the Curie-Weiss law for all the orthorhombic axes. The high Neel temperature $T_N = 114$ K and the absence of the broad maximum of susceptibility above the Neel temperature suggest that the $PbFeBO_4$ crystal is a three-dimensional antiferromagnet.

The magnetic susceptibility anisotropy in the ordered state indicates that the antiferromagnetic vector is directed along the orthorhombic $\boldsymbol{c}$ axis. The exchange field estimated from the field dependence of magnetization is $H_E = 1.3 \times 10^6$ Oe at $T = 2$ K.

The anomalies of permittivities ε' and ε'' were observed in both polycrystalline and single-crystal samples within the temperature ranges where the short- and long-range magnetic orders are established. This confirms the correlation between the dielectric and magnetic subsystems in the crystal.

Acknowledgments

This work was supported by RFBR, Grant no. 13-02-00897.

References

[1] G.A. Petrakovskii, K.A. Sablina, A.M. Vorotinov, V.N. Vasiliev, A.I. Kruglik, A.D. Balaev, D.A. Velikanov, N.I. Kiselev, Sol. State Commun. 79 (1991) 317.
[2] G. Petrakovskii, D. Velikanov, A. Vorotinov, A. Balaev, K. Sablina, A. Amato, B. Roessli, J. Schefer, U. Staub, J. Magn. Magn. Mater. 205 (1999) 105.
[3] G.A. Petrakovski, K.A. Sablina, A.I. Pankrats, O.A. Bayukov, V.I. Tugarinov, A.M. Vorotinov, A.D. Vasiliev, G.V. Romanenko, Yu.G. Shvedenkov, Phys. Solid State 44 (2002) 1339.
[4] G.A. Petrakovski, M.A. Popov, A.D. Balaev, K.A. Sablina, O.A. Bayukov, D.A. Velikanov, A.M. Vorotinov, A.F. Bovina, A.D. Vasiliev, M. Boehm, Phys. Solid State 51 (2009) 1866.
[5] A.D. Balaev, N.V. Volkov, N.V. Sopronova, K.A. Sablina, A.D. Vasiliyev, J. Phys.: Condens. Matter 21 (2009) 336006.
[6] H. Park, R. Lam, J.E. Greedan, J. Barbier, J. Chem. Mater 15 (2003) 1703.
[7] N.A. Toropov, V.P. Barzakovskii, V.V. Lapin, N.N. Kurtseva, State Diagrams of Silicate Systems, Reference Book, Nauka, Moscow-Leningrad, 1965.
[8] H. Park, J. Barbier, Acta Crystallogr E57 (2001) 82.
[9] J.O. Artman, J.C. Murphy, S. Foner, Phys. Rev. 138 (1965) 912.
[10] R.C. Wayne, D.H. Anderson, Phys. Rev. 155 (1967) 496.
[11] P.J. Besser, A.H. Morrish, C.W. Searly, Phys. Rev. 153 (1967) 632.
[12] P.J. Flanders, J.P. Remeika, Philos. Mag. 11 (1965) 1271.
[13] B.Ya.Kotyuzhanskii, M. Maryshko, L.A. Prozorova, JETP 50 (1979) 386.
[14] G.A. Petrakovskii, A.I. Pankrats, V.M. Sosnin, V.N. Vasil'ev, J. Exp. Theor. Phys. 58 (1983) 403.
[15] C.R. Nininger, D. Schroeder, J. Phys. Chem. Solids 39 (1978) 137.
[16] A.S. Borovik-Romanov, V.I. Ozhogin, Zhurnal Eksperimental'noy i Teoreticheskoy Fiziki 39 (1960) 27.
[17] A. Gauzzi, E. Gilioli, A. Prodi, F. Bolzoni, F. Licci, M. Marezio, G.L. Galestani, M. Affronte, Q. Huang, A. Santoro, J. Lynn, J. Supercond.: Incorporating Novel Magn. 18 (2005) 675.
[18] Y.A. Park, K.M. Song, K.D. Lee, C.J. Won, N. Hur, Appl. Phys. Lett. 96 (2010) 092506.
[19] G. Lawes, A.P. Ramirez, C.M. Varma, M.A. Subramanian, Phys. Rev. Lett. 91 (2003) 257208.
[20] T. Katsufuji, S. Mori, M. Masaki, Y. Moritomo, N. Yamamoto, H. Takagi, Phys. Rev. B64 (2001) 104419.
[21] T. Kimura, S. Kawamoto, I. Yamada, M. Azuma, M. Takano, Y. Tokura, Phys. Rev. B67 (2003) 180401.